

Title: Maternal Hypothyroxinemia impairs Spatial Learning and Synaptic nature and function in the Offspring

Short title: Hypothyroxinemia impairs offspring cognition

Authors: ¹Opazo MC, ¹Gianini A, ²Pancetti F, ³Azkcona G, ¹Alarcón L, ¹Lizana R, ¹Noches V, ^{4,5}Gonzalez PA, ⁶Porto M, ⁷Mora S, ⁶Rosenthal D, ⁸Eugenin E, ⁹Naranjo D, ^{4,5}Kalergis AM and ¹Riedel CA.

Affiliations:

¹ Laboratorio de Biología Celular y Farmacología, Departamento de Ciencias Biológicas, Universidad Andrés Bello, Santiago, Chile. ² Laboratorio de Neurotoxicología Ambiental. Departamento de Ciencias Biomédicas, Facultad de Medicina, Universidad Católica del Norte, Coquimbo, Chile. ³ Faculty of Medicine, Department of Neuroscience, Universidad del País Vasco, España. ⁴ Millennium Nucleus on Immunology and Immunotherapy, Departamento de Genética Molecular y Microbiología, Facultad de Ciencias Biológicas. ⁵ Departamento de Reumatología, Facultad de Medicina, Pontificia Universidad Católica de Chile. ⁶ Instituto de Biofísica Carlos Chagas Filho of Federal University of Rio de Janeiro, Brazil. ⁷ Instituto de Ciencias Biomédicas, Facultad de Medicina Universidad de Chile, Chile. ⁸ Department of Pathology, Albert Einstein College of Medicine, USA. ⁹ Centro de Neurociencias de Valparaíso, Facultad de Ciencias, Universidad de Valparaíso, Chile.

Corresponding author: Dr. Claudia Riedel, Laboratorio de Biología Celular y Farmacología, Departamento de Ciencias Biológicas, Universidad Nacional Andrés Bello, República 217 Santiago, Chile. Phone: 56-2-6618419. email: riedel@unab.cl

Reprints should be addressed to: Dr. Claudia Riedel Laboratorio de Biología Celular y Farmacología, Departamento de Ciencias Biológicas, Universidad Nacional Andrés Bello, República 217 Santiago, Chile

Keywords: Maternal hypothyroxinemia, learning, postsynaptic densities.

Grant: FONDECYT # 1040349

DISCLOSURE STATEMENT: The authors have nothing to disclose.

ABSTRACT

Neurological deficits in the offspring caused by human maternal hypothyroxinemia are thought to be irreversible. To understand the mechanism responsible for these neurological alterations, we induced maternal hypothyroxinemia in pregnant rats. Behavior and synapse function were evaluated in the offspring of thyroid hormone-deficient rats. Our data indicate that, when compared to controls, hypothyroxinemic mothers bear litters that, in adulthood, show prolonged latencies during the learning process in the water maze test. Impaired learning capacity caused by hypothyroxinemia was consistent with cellular and molecular alterations including (1) lack of increase of phosphorylated c-Fos on the second day of the water maze test; (2) impaired induction of long-term potentiation in response to theta-burst stimulation to the Schaffer collateral pathway in the area 1 of the hippocampus Ammon's horn stratum radiatum, despite normal responses for input/output experiments; (3) increase of postsynaptic density-95, N-methyl-D-Aspartic Acid receptor subunit 1, and tyrosine receptor kinase B levels in brain extracts; and (4) significant increase of postsynaptic density-95 at the postsynaptic densities and failure of this molecule to colocalize with N-methyl-D-Aspartic Acid receptor subunit 1, as it was shown by control rats. Our findings suggest that maternal hypothyroxinemia is a harmful condition for the offspring that can affect key molecular components for synaptic function and for spatial learning.

INTRODUCTION

Maternal hypothyroxinemia is a pathological condition that induces cognitive impairment in the progeny. A number of reports, derived from human studies, have shown that there is a strong correlation between maternal hypothyroxinemia and cognitive damage in the offspring. These studies reported that 50% of the offspring gestated in hypothyroxinemic mothers show neuronal damage [1-5]. A hypothyroxinemic patient is characterized by having low serum levels of tiroxine (T_4), and normal levels of triiodothyronine (T_3) and thyroid-stimulating hormone (TSH) [1]. Maternal hypothyroxinemia is an asymptomatic condition for the mother, but it is extremely harmful for the fetus. Because the fetus's thyroid is still too immature to synthesize sufficient T_3 and T_4 , thus the fetus relies on the maternal thyroid hormone for its optimal brain development. Brain damage in the offspring caused by maternal hypothyroxinemia is considered to be irreversible and characterized by attention deficit, low intelligence quotient (IQ), and mental retardation [6,7]. However, the molecular mechanisms responsible for the cognitive damage caused by hypothyroxinemia remain unknown. Recent studies have shown that (1) maternal hypothyroxinemia can alter the cellular architecture of the somatosensory cortex and hippocampus of the offspring [8]; (2) 83% of the offspring had deficient radial migration of projection neurons [9]; (3) maternal hypothyroxinemia also alters tangential migration of medial ganglionic eminence-derived neurons of the progeny [10]. Nevertheless, the previously described alterations caused by maternal hypothyroxinemia failed to explain all the features of cognitive deficiency caused by hypothyroxinemia in the offspring. Given that maternal hypothyroxinemia is highly prevalent in humans [1], here we have evaluated some of the cellular and molecular alterations caused by this disorder in the offspring's brain. As a model, we used methimazole (MMI) treatment to develop hypothyroxinemia in pregnant rats [9] and followed up the offspring to adulthood. To assess cognitive deficiencies in the progeny gestated in hypothyroxinemic mothers, their

behavior was evaluated and compared to that of control animals. We found that maternal hypothyroxinemia caused significant cognitive damage to the offspring, manifested as impaired spatial learning behavior. These animals showed impaired responses of collateral-schaffer in the area 1 of hippocampus Ammons's horn (CA1) synapsis of the hippocampus to theta-burst stimulus (TBS), which are required for efficient learning and memory processes. Contrarily to what was observed in control rats, the content of phosphorylated c-Fos failed to increase in the MMI offspring subjected to spatial learning tests. C-Fos is an immediate early gene (IEG) essential for appropriate spatial learning behavior in these animals [11-14]. Finally, analyses of the protein content of excitatory neurons postsynaptic densities (PSD) revealed an abnormal increase of proteins that are critical for synaptic function. Our data suggest that maternal hypothyroxinemia in rats can severely impair the learning capacity of their progeny and that this cognitive damage could be due to physiological and molecular alterations at glutamatergic synapses.

MATERIALS AND METHODS

Animals and treatments

Young female adult Sprague-Dawley rats were maintained at 22°C in a room with automatic light/dark cycles of 12/12 h. Female rats weighing ~ 250 g were mated and next day a vaginal smear was obtained and analyzed under microscope to search for spermatozoa. Rats with smear positive for spermatozoa were considered mated and one day post-mating was referred as embryonic day 0 (E0). Pregnant rats were separated randomly in two groups. A group of pregnant rats (n=6) was transiently treated with 2-mercapto-1-methylimidazole (methimazole MMI) as described previously [9]. Briefly, 0.02% of MMI was added to the drinking water during E12–E15. Control animals (n=6) received the same drinking water but without MMI. After MMI treatment (E15), blood samples were collected from the tail and sera were analyzed for hormone levels. The day of birth was referred as postnatal 0 (P0). The offspring from MMI treated (MMIo) and control were weaned at P30 and culled to perform the experiments at P60. Pregnant dams used for hormone determination were n=6 both for MMI and controls. TSH determination was performed on MMI (n=3) and control (n=2) animals. Rats used for water maze test were n=16 for MMIo and n=17 for controls. Rats used for the visible-platform test were n=3 for MMIo and n=3 for controls. Dams used for visible-platform tests had been subjected to water maze test two weeks before. The following experiments were done with new dams. Rats used for extracellular field recording and LTP induction assays were: n=9 for MMIo and n=6 for controls. Western blot analyses were performed for 3 independent experiments, both for PSD and brain homogenates. The number of dams used for each experiment was n=10 for MMIo and n=10 for control. The number of rats used for western blots analysis of c-Fos and phosphorylated c-Fos was n=3 for MMIo and n=3 for controls. The number of rats used for BDNF determination was: MMIo (n=10) and control (n=10). The number of rats used for immunofluorescence analyses was n=3 for MMIo and n=3 for controls. Dams used for BDNF determination and c-Fos analyses were used as well for

western blot analyses of PSD and brain homogenates.

Hormone determination

Plasma levels of TSH were measured by radio-immune assay (RIA) at the Instituto de Biofísica Carlos Chagas Filho of Federal University of Rio de Janeiro, Brazil [15]. Plasma levels of total T₃ (tT₃) and free T₄ (fT₄) were measured by chemiluminescence in the laboratory of Instituto de Estudios Médicos Avanzados (IEMA), Santiago, Chile [16]. Thyroid hormones levels resulting from our assays on rat sera were equivalent to those previously reported in the literature [9,17]

Water maze test

The water maze test used in our experiments was described by Richard Morris in 1984 [18]. This method is used to assess spatial learning and memory in rodents. The apparatus consists of a black circular swimming pool (150 cm diameter, 50 cm depth) that was filled with water (22° C temperature) to 20 cm below the rim. The pool was divided into four quadrants of equal area. Each area was arbitrarily called north, south, east, and west. A circular plexiglas platform (10 cm diameter) was located 2 cm below the water surface in the middle of the north quadrant. This platform had the same color as the swimming pool in order not to be visualized by the rat. The procedure room, where the swimming pool was located, had spatial cues on the walls for spatial orientation.

The water maze test was performed at P60. The entire procedure took 5 d and rats were moved to the procedure room 30 min prior to testing. Each rat had five training trials per day, with 20-min inter-trial intervals. The two investigators that worked with the water maze procedure were always the same and located always at the same position in the room. On each trial, the rat was placed into the water, immediately facing the perimeter of the pool at one of the cardinal compass points (north, south, east, or west), and was allowed to locate the platform with a maximal time of 120 s. The time spent by the rat to find the platform was recorded and assigned as latency. After staying on the platform for 20 s, the rat was gently picked up, returned to its home cage, and

allotted to warm up and dry off under a heat lamp. If the rat failed to find the platform in the allowed time, it was placed onto the platform for 30 s and was assigned a latency of 120 s. Cue task training test, a control to assess the motor and visual capacity of rodents, was performed two weeks after the water maze test. This test is a visible-platform test, where the platform was 2 cm above the water and the rest of the procedure was exactly the same as in the above invisible platform. Results were expressed as the mean + standard error of the mean (SEM) of the latencies measured on each day for each group. Statistical analyses for the water maze tests were performed on each day latencies derived from control and MMio animals. Analyses were performed using the Mann-Whitney test. Data from the visible platform test were analyzed by unpaired t-test. The Sigma Plot9 plus sigma Stat 3.5 program (Systat Software, Inc.) was used for the analyses. Data were considered statistically significant when *P* was equal to or less than 0.05.

Extracellular field recording and long-term potentiation (LTP) induction

Transverse hippocampal slices of MMio and control rats were prepared for extracellular field recording and long term potentiation (LTP) assays. Animals were anesthetized with halothane gas and decapitated soon after the disappearance of any corneal reflexes. Brains were rapidly removed and immersed in ice-cold dissection buffer containing 212.7 mM sucrose, 5 mM KCl, 1.25 mM NaH₂PO₄, 3 mM MgSO₄, 1 mM CaCl₂, 26 mM NaHCO₃, and 10 mM glucose at pH 7.4. Hippocampi were dissected free and transverse slices (400 μm thick) were obtained from the middle third portion using a vibratome (Model HA752, Campden Instruments, Leicester, England). Slices were transferred to an interface storage chamber containing artificial cerebro-spinal fluid (ACSF) saturated with 95% O₂ / 5% CO₂ and left for at least 1 h at 37 °C before recording. ACSF contained 124 mM NaCl, 5 mM KCl, 1.25 mM NaH₂PO₄, 1.0 mM MgCl₂, 2.0 mM CaCl₂, 26 mM NaHCO₃, and 10 mM glucose at pH 7.4. Single slices were then transferred to a recording chamber, where they were kept completely

submerged in ACSF and continually perfused (2 ml/min).

Field excitatory postsynaptic potentials (fEPSPs) were evoked with electrical stimulation delivered every 15 s to the Schaffer collateral pathway using bipolar electrodes and recorded in the *stratum radiatum* (for measuring fEPSP slopes) of the CA1 hippocampal area. Recording electrodes were glass micropipettes (1-3 MΩ) filled with ACSF. At the beginning of each experiment, stimulus/response (input/output) curves were obtained by increasing the intensity of the stimulus in order to adjust it to elicit 50% of the maximal response. LTP was elicited after 10 min of a stable baseline by theta-burst stimulation (TBS) consisting of three trains with an inter-train interval of 10 s. Each train of 10 was made up by bursts at 5 Hz and each burst had four pulses at 100 Hz separated by 200 ms. After TBS, data acquisition continued for 30 min. Data were acquired using a differential alternating current amplifier (Model 1800, A-M Systems Microelectrode, USA) and a data acquisition card (National Instruments, USA) controlled through IGOR software (Wavemetric Inc, USA).

Determination of proteins from homogenate and PSD

PSDs and homogenate were isolated from the telencephalon to analyze the presence and amounts of some specific proteins in this structure and fraction respectively. The PSD fraction was isolated from the rest of the homogenate, as previously described [19]. Briefly, MMio and control male rats at P60 were decapitated and their brains isolated. The cerebral cortex and hippocampus (telencephalon) were dissected, cut, and homogenized on ice in 8 ml of homogenization buffer (0.32M sucrose, 0.5mM EDTA, 5mM Tris pH 7.4), using 12 strokes with a 40 ml Tissue Grind Potter with Teflon Pestle (Thomas Scientific). One ml of the homogenate was saved to be analyzed for total protein concentration. Then, the telencephalon homogenate was centrifuged at 1000xg for 10 min at 4°C (Sorvall 5B-plus, SS-34 rotor). The supernatant (S1) was saved. The pellet (P1) was washed, manually homogenized, and centrifuged at 1000xg for 10 min at 4°C. The pellet (P2) was

discarded and the supernatant (S2) was mixed with S1. S1+S2 were centrifuged at 12000xg (Sorvall 5B-plus, SS-34 rotor) for 20 min at 4°C. The pellet (P3) was saved and rinsed with solution A (0.32 Sucrose, 5 mM Tris-HCl pH8.1, 0.5mM EGTA, and 1mM dithiotreitol). Then, the P3 was manually homogenized with a 17 ml Tissue Grind Potter with Teflon Pestle (Thomas Scientific) and layered on a discontinuous sucrose step gradient (0.32M, 1M, 1.2M sucrose in 5mM Tris-HCl pH 8.1) and centrifuged at 150000xg using the AH629 rotor (Sorvall) for 2 h at 4°C. The synaptosome 1 fraction (Syn1) was isolated from 1 to 1.2 M sucrose gradient and diluted 10 times its volume with the lysis buffer (5mM Tris-HCl pH (8.1) and 0.5 EGTA). The lysis was performed by incubating and gently mixing the lysis buffer with Syn1 in ice for 30 min. Then Syn1 was centrifuged at 33.000xg for 30 min (Sorvall RC5B plus rotor SS34). The pellet (P4) was saved, resuspended in 3 ml of solution A, and manually homogenized. Then P4 was layered on a discontinuous sucrose step gradient (0.32M, 1M, 1.2M sucrose in 5mM Tris-HCl pH 8.1) and centrifuged at 250000xg using the TH660 rotor (Sorvall) for 1 h at 4°C. The fraction of synaptosomes 2 (Syn2) was obtained from 1 M and 1.2 M fractions. Syn2 was saved and diluted with 8 volumes of 0.32M Sucrose, 0.025 mM CaCl₂, 1% Triton X-100, 2 mM DTT, and 10mM Tris-HCl pH 8.1. Then, the Syn2 was gently mixed in this buffer and centrifuged at 33000xg (Sorvall RC5B plus rotor SS34) for 30 min at 4°C. The pellet (P5) is the PSD fraction. It was saved and washed with 50 mM HEPES pH 7.4. The PSDs were centrifuged at 250000xg (Beckman Optima TLX, rotor TLA110) for 10 min at 4°C and the pellet was resuspended in 50 mM HEPES pH 7.4. The PSD fraction was frozen in liquid nitrogen and stored at -80°C.

Protein concentration in the PSD fraction and total telencephalon homogenate samples was determined by the bicinchoninic acid method [20]. The PSD and total homogenate samples were diluted 1:1 with loading buffer and heated at 100°C for 5 min. Then, 20 µg and 40 µg of protein, respectively, was loaded on a 10% SDS-PAGE, separated by electrophoresis, and electrotransferred to nitrocellulose sheets that were incubated one at a

time with (1) anti-NR1 antibody (Chemicon catalog number AB1516) 1/1000 dilution incubated for 1 h [21]; (2) anti-NR2 A/B antibody (Chemicon catalog number AB1548W) 1/2000 dilution incubated for 1.5 h [21]; (3) anti-P75 antibody (Upstate catalog number 07-476) 1/1000 dilution incubated for 1h [22]; (4) anti-PSD-95 antibody (Chemicon catalog number MAB377) 1/1000 dilution incubated for 16 hours [23]; (5) anti-TrkB antibody (Transduction catalog number 610102) 1/1000 dilution incubated for 16 h [24]; (6) anti-TrkA antibody (Santa Cruz Biotechnology catalog number SC-14024) 1/200 dilution incubated for 16 h [25]; (7) anti-CAMKII antibody (Upstate catalog number 05-533) 1/2000 dilution incubated for 16 h [26]; (8) anti-phosphorylated c-Fos antibody (Abcam catalog number ab17933) 1/300 dilution incubated for 16 h, which is directed to phospho T232 of c-Fos [27]; (9) anti-c-Fos antibody (Calbiochem catalog number PC05L) 1/100 dilution incubated for 16 h [28]; and (10) anti-Actin antibody (Abcam catalog number ab1428) 1/1000 dilution incubated for 16 h (data sheet Abcam). A horseradish peroxidase-linked goat anti-rabbit IgG (Calbiochem, catalog number 401215) or horseradish peroxidase-linked goat anti-mouse IgG (Calbiochem, catalog number 401315) was used as secondary antibody. Both of these secondary antibodies were diluted to 1/1500 and incubated with the nitrocellulose for 1 h. For c-Fos and phosphorylated c-Fos, the secondary antibody was peroxidase-linked horseradish anti-rabbit (Jackson, catalog number 115-035-003) diluted to 1/25000 in Tween-20 10%, BSA 5%, 150 mM NaCl, 10 mM Tris pH 8.0 (TBST). The nitrocellulose was washed and then incubated with the enhanced chemiluminescence (ECL) Western blot detection system (Amersham) to visualize the proteins.

Brain-derived neurotrophic factor (BDNF) determination

The content of BDNF was analyzed using 7 mg of the total telencephalon homogenate. The homogenate was centrifuged at 14000 rpm in a MIKRO 22R Hettich Zentrifuge at 4°C for 30 min. The supernatant was discarded and the pellet was lysed in 137 mM NaCl, 20 mM Tris-HCl (pH 8.0), 1% NP40,

10% glycerol, 1mM of PMSF, 10 µg/ml aprotinine, 1µg/ml leupeptine, and 0.5 mM sodium vanadate. The samples were sonicated with three pulses for 15 s at intensity 4 with 5-s intervals in a Misonix Sonicator Ultrasonic processor XL. After sonication, samples were centrifuged at 16000 rpm for 30 min at 4°C in a MIKRO 22R Hettich Zentrifuge. Aliquots of 100 µl of the supernatants were isolated and mixed with 40 µl of 137 mM NaCl, 2.68 mM KCl, 1.47 mM KH₂PO₄, 8.1 mM Na₂HPO₄ (pH 7.35), 0.9 mM CaCl₂, and 0.5 mM MgCl₂. Then these were treated with 20µl of HCl 1 N for 15 min and neutralized with 20 µl of 1 N of NaOH. The samples were kept at -80°C. The content of BDNF in the extracts was analyzed by BDNF Emax ® Immunoassay System (Promega) as described [29]. Briefly, a 96-well plate was covered with anti-BDNF monoclonal antibody. To allow the antibody to stick to the well, 100 µl of 1:1000 diluted antibodies was added to the well and left overnight at 4°C. Then, the plate was washed with 150 mM NaCl, 0.05% Tween 20, and 20 mM Tris-HCl (pH7.6) and was blocked with 200 µl of Promega 1X blocking solution and sample buffer for 1 h. Plates were then washed with the TBST buffer, and 100 µl of sample or BDNF standard was added in triplicate to each well and incubated for 2 h at 4°C. Then the plate was washed five times using TBST buffer and 100 µl of anti-human BDNF polyclonal antibody diluted to 1:500 was added to each well of the plate and incubated for 2 h. The plate was again washed with TBST buffer and incubated with 100 µl of 1:200 dilution of anti-IgY horseradish peroxidase conjugate for 1 h at room temperature. The plate was washed with TBST buffer and developed with 100 µl Promega TMB solution. This reaction was stopped with 100 µl of 1N HCl. The absorbance was measured at 450 nm. The BDNF concentration was expressed as pg of BDNF/ mg of protein.

Immunofluorescence

Telencephalons obtained from decapitated rats were covered with OCT, then frozen with cold isopentane (Merck) and immediately treated with liquid nitrogen for two minutes. Using a cryostat (Leica, CM 1510), 30

µm coronal sections were obtained from these telencephalons. The sections were fixed and permeabilized in 70% ethanol for 20 min at -20°C. Sections were incubated in blocking solution (5 mM EDTA, 1% fish gelatin, 2% horse serum, and 1% essentially immunoglobulin-free BSA) for 30 min at room temperature. Sections were then incubated in primary antibody overnight at 4°C at the following concentrations: anti-NMDAR1 (NR1, rabbit polyclonal, 1:50, Sigma) and anti-PSD-95 (goat polyclonal, 1:300, Santa Cruz). Fixed sections were washed four times with PBS, incubated with FITC-conjugated goat anti-rabbit IgG and Cy3-conjugated sheep anti-goat IgG (1:300) for 1 h at room temperature, followed by another wash in PBS for 1 h. Coverslips were then mounted using Prolong Gold with DAPI (Molecular Probes) and examined by confocal microscopy using a Leica Microscope. Specificity immunoreactivity was confirmed by replacing the primary antibody with a nonimmune polyclonal reagent [30]. To analyze colocalization of both antigens by confocal microscopy, serial Z-sections from the sections were obtained (0.8 fÝm each section) and all sections were integrated using Image J, Voxx, and Adobe Photoshop programs.

Statistical analyses

Unpaired two tailed t-tests were performed on the experimental data shown here. The Sigma Plot9 plus sigma Stat 3.5 program (Systat Software, Inc.) was used for the analyses. The results were considered to be significantly different when $P < 0.05$.

RESULTS

Methimazole treatment causes hypothyroxinemia in pregnant rats

Pregnant rats were treated with MMI during E12–E15 to induce transient and mild hypothyroxinemia, as described previously [9,10] and detailed in the Methods section. Hypothyroxinemia was confirmed by determining plasma levels of fT_4 , tT_3 , and TSH at the end of the MMI treatment (day E15). The MMI treatment showed a significant reduction in fT_4 as compared to control rats (MMI 0.788 ± 0.201 ng/ml; control 3.107 ± 0.578 ng/ml; SEM $N=6$; $P<0.05$; Fig. 1A). No significant differences were observed for tT_3 (MMI 60 ± 10.062 ng/dl; control 40.7 ± 0.5 ng/dl; SEM $N=6$; Fig. 1B) or for TSH (MMI 2.48 ± 0.5378 ng/dl $N=3$; control 2.8 ± 0.5672 ng/dl; SEM $N=4$; Fig. 1C). The reduction observed only for the fT_4 plasma level indicated that pregnant rats treated with MMI developed hypothyroxinemia.

Maternal hypothyroxinemia leads to spatial learning impairment in adult offspring

To evaluate whether maternal hypothyroxinemia could cause cognitive and behavioral alterations in the offspring, a water maze test was performed on its progeny (MMIo) mothers or control dams. Controls consisted of male progeny from dams that were not exposed to MMI and that had normal levels of thyroid hormones and TSH (Fig. 1). Significant differences were observed between the MMIo and control animals in the water maze test (Fig. 2). This test was performed during five consecutive days with five trials per day. In each trial, the rat was left in the water and the time (latency) needed for the rat to reach the hidden platform was recorded. On the first day, MMIo and control rats had latencies between 60–70 s, indicating that none of the groups had swimming impediments (Fig. 2). Importantly, from day 2 to 4, significantly higher latencies were observed for the MMIo group, as compared to controls (Fig. 2A). These data are consistent with the notion that MMIo animals are slower than the controls at finding the platform. However, on day 5, latencies of MMIo and control animals showed no significant differences, suggesting that MMIo rats needed more time and/or experience to learn the spatial cues required to

find the hidden platform than the controls (Fig. 2A). It seems unlikely that the learning delay shown by MMIo rats could be due to visual perception defects, because MMIo and control rats showed equivalent latencies during a 3 day water maze test with a visible platform (cued task training) (Fig. 2B). Therefore, because MMIo rats had no apparent visual perception defects, our data suggest that maternal hypothyroxinemia during gestation may have impaired the inner capacity of the offspring to learn the location of the hidden platform using spatial orientation.

Content of phosphorylated c-Fos post-water maze test was unaffected in adult offspring gestated by hypothyroxinemic mothers.

c-Fos is an immediate early gene (IEG) required for spatial learning [11-14], whose expression in rat brain increases during water maze test training [14]. An important posttranscriptional regulatory mechanism for c-Fos activity is phosphorylation, which is required to keep active c-Fos in the nucleus and for the assembly of a stable AP-1 complex [31-33]. Thus, we tested whether the telencephalon content of c-Fos and phosphorylated c-Fos could increase in the MMIo group as compared to controls on day 2 of the water maze test (time when MMIo latencies were significantly longer than those of the controls). Also, content of c-Fos and phosphorylated c-Fos was also evaluated for MMIo and control rats not subjected to the water maze test.

Western blot analyses showed an increase in the relative content of phosphorylated c-Fos in control rats on day 2 of the water maze test (normalized for actin content) (Fig. 3A). In striking contrast, MMIo rats showed no significant changes for content of either c-Fos or phosphorylated c-Fos after 2 days of water maze testing (Fig. 3A and 3B). These data are consistent with the longer latencies shown by MMIo rats at day 2 of the water maze test.

MMI treatment alters LTP in adult offspring

Because long term potentiation (LTP) at the hippocampus is required for cognitive processes, such as spatial learning [34,35], we tested whether long latencies shown by MMIO rats during water maze tests could be due to LTP alterations caused by hypothyroxinemia. Furthermore, in order to establish if MMI treatment affect the synaptic efficacy of the Schaffer collateral → CA1 pathway, input/output ratios were measured in response to single electrical stimulation, comparing between control and MMIO. fEPSP responses elicited by stimulus strength intervals of 20 μ A were measured at the CA1 *stratum radiatum* area. When stimulus strength reached 100 μ A, increments were added on steps of 50 μ A up to a 500 μ A maximum. Three responses were collected and averaged for each stimulus increment. To construct input-output curves (Fig. 4A), data were averaged across all slices measured for each group (control and MMIO). These assays showed no significant differences between control and MMIO groups, suggesting that these two groups had similar synapse densities at the *stratum radiatum* of CA1 and displayed equivalent excitability in response to single electrical stimulation.

To evaluate a possible effect of MMI treatment on the mechanisms of synaptic plasticity, we performed LTP experiments consisting of recordings of stimulus-evoked fEPSPs in the *stratum radiatum* of CA1 of hippocampal slices obtained from Co and MMIO rats. A 10 min stable baseline transmission was obtained and tested it every 15 s. Following baseline acquisition, TBS was applied as described in Materials and Methods. After stimulation, data was acquired once every 15 s for at least 30 min. Data from several experiments were aligned relative to the time of TBS stimulation for Co and MMIO animals (Fig. 4B). For control rats, $178 \pm 16\%$ (SEM, n=9) potentiation was achieved with respect to the baseline. In contrast, for MMIO rats potentiation was significantly smaller $130 \pm 3\%$, (SEM, n=6). Representative traces of fEPSPs observed before and after LTP induction for control and MMIO animals are shown in Figure 4C. These results indicate that MMI treatment during gestation significantly impair the LTP response.

Maternal hypothyroxinemia promotes an increase of PSD proteins

Considering the MMIO group had impaired LTP and that hippocampus glutamatergic synapses play an essential role during this process [36], their PSD protein composition was analyzed. The following PSD proteins fundamental for the transmission of glutamatergic synapses were studied: (1) The subunits of the N-methyl-D-aspartate (NMDA) receptor (NR1 and NR2A/B); (2) The postsynaptic density protein 95 (PSD-95); (3) The calmoduline kinase II (CaMKII); (4) The tyrosine receptor kinase B (TrkB) and its ligand, BDNF; (5) The tyrosine receptor kinase A (TrkA) and (6) The receptor P75.

The content of all these proteins was analyzed both in the PSD fraction and total telencephalon homogenates. Representative western blots for each protein are shown in Figure 5A. To evaluate the unspecific binding of the secondary antibodies, all membranes were incubated with only the second antibodies. No bands were detected indicating that all the bands shown in Figure 5A correspond to the first antibody reaction and not to nonspecific binding of the secondary antibody. Standardization of the loaded amount of protein per well was performed by using actin as a loading control both for PSD and total telencephalon homogenate. The anti-actin antibody recognized a 43 kDa band. No significant differences were found between the content of actin from the MMIO group as compared to the Co group, both in the PSD and the total telencephalon homogenate, indicating that the same amount of total protein was loaded for all samples (Fig. 5A). For PSD-95 and TrkB, densitometry analyses showed a significant increase in the content of these proteins in both PSD and total telencephalon homogenate of MMIO relative to control group. For PSD95 (95 kDa band [23]), densitometry analyses showed a $40 \pm 0.7\%$ increase in total MMIO telencephalon homogenates, as compared to control animals ($P < 0.05$, n=3). An equivalent PSD-95 increase was also observed in the PSD samples of MMIO rats, relative to controls ($P < 0.05$ n=3). TrkB (145 kDa band, [24]), in the PSDs of the MMIO showed an increase of $10 \pm 1.73\%$ ($p < 0.01$) as compared to Co. TrkB in the total telencephalon

homogenate showed an increase of $15 \pm 5.29\%$ ($p < 0.05$) in the MMI relative to control. The total levels of BDNF (TrkB ligand) from telencephalon were analyzed by ELISA (Fig. 5B). Even though the control group had a larger BDNF content (108 ± 72 pg/mg of protein) than the MMIO group (47 ± 15 pg/mg of protein), this disparity was not statistically significant. For NR1 (120 kDa band, [21]), densitometry analyses showed no significant differences between control and MMIO rats in the NR1 content at PSD ($1 \pm 4.62\%$, $n=3$). However, a significant increase (3.5 fold) of NR1 content was observed in total telencephalon homogenates from MMIO rats ($35 \pm 10\%$; $P < 0.05$; $n=3$) as compared to control rats (Figure 5A). For NR2A/B (180 kDa band, [21]), CaMKII (33 kDa band [26], TrkA (140 kDa band, [25]) and p75 (75 kDa band [22]), densitometry analyses showed no significant differences either in the PSD or the total telencephalon homogenates. We observed an increase in the content of p75 in the PSD and total telencephalon homogenate of the MMIO compared to controls ($10 \pm 29.9\%$ and $10 \pm 61.5\%$ respectively); however, these increases were not statistically significant.

Offspring of hypothyroxinemic dams showed a different distribution of PSD-95 and NR1 in the CA1 hippocampus.

PSD-95 and NR1 are two key players in PSDs, because they contribute significantly to cognitive processes, such as synaptic plasticity and learning. Considering that Schaffer collateral-CA1 synapses showed an impaired LTP response and that expression of PSD-95 and NR1 was elevated in total telencephalon homogenates, it was important to evaluate the localization of these two proteins in the hippocampus CA1 area. Thus, localization of NR1 and PSD-95 was analyzed by confocal microscopy in coronal brain sections of 30 μm obtained from control and MMIO rats (Figure 6). NR1 and PSD-95 showed significant colocalization and a punctuated pattern in hippocampi of control rats. However, a different NR1 and PSD-95 distribution was observed in the hippocampuses of MMIO rats. The hippocampus of these animals showed a stronger PSD-95 staining than control rats. Furthermore,

PSD-95 staining appeared more concentrated forming large aggregated structures in the hippocampus. Although a punctuated pattern was also observed for PSD-95 in MMIO rats, this was very different from that in control rats. PSD-95 spots in MMIO hippocampi were clustered and looked more diffused and less bright than in controls. In addition, the NR1 stain in MMIO rats was concentrated mainly in big aggregated structures with few bright spots, which was very different from the pattern observed in control animals. Finally, in MMIO rats, PSD-95 and NR1 colocalization was restricted to the aggregated structures detected in the hippocampus.

DISCUSSION

It has been reported that maternal hypothyroxinemia in humans can cause irreversible cognitive damage to the progeny [1,6,7]. To further understand the alterations that are responsible for these cognitive impairments, we analyzed several molecular and functional parameters in the neurons from the telencephalon and characterized the cognitive capacity of the offspring from rats with hypothyroxinemia [9]. Two studies had previously reported that effects induced in the offspring of hypothyroxinemic dams can be reversed by the administration of T_4 to the pregnant rats during the MMI treatment [9,10]. Here, mild maternal hypothyroxinemia was induced in pregnant rats by a 4 d treatment with MMI, which led to reduced plasmatic levels of fT_4 without affecting significantly the plasmatic levels of tT_3 and TSH. Neither the outcome of the pregnancy nor the survival and weight of the offspring was affected by the MMI treatment. All experimental procedures were performed on offspring at the age of P60, because at this age rats are considered to be adults and their brain synapses are mature and functional. Our data show for the first time that maternal hypothyroxinemia can cause in the offspring a significant reduction in the capacity of the brain for spatial learning. MMIO rats systematically showed impaired performance in water maze tests, as demonstrated by significantly extended latencies during testing on the second, third, and fourth days (Fig. 2). However, the observation that by day 5 MMIO rats reached the platform with the same latencies as the controls, suggests that MMIO rats need to experience the event more times for establishing or reinforcing the appropriate neuronal connections required for spatial learning. Considering that no significant differences were observed between MMIO and control rats in other behavior tests, such as the elevated plus maze test and the passive avoidance test, it seems likely that maternal hypothyroxinemia leads specifically to a deficiency in spatial learning, rather than other type of behavioral alterations.

To better understand the molecular alterations in the brain of MMIO rats that could lead to an impaired performance in water maze

tests, the content of c-Fos and phosphorylated c-Fos was analyzed. C-Fos is an IEG involved in spatial learning [11-14]. While experiencing the water maze test led to a significant increase in the telencephalon content of phosphorylated c-Fos in control rats, no significant increase was seen in MMIO rats exposed to the test (Figs. 3A and B). Our data agree with findings suggesting a relationship between spatial learning and phosphorylated c-Fos content in the telencephalon.

Given that hippocampus synapses play an important role during water maze training [37-40] and are required for a proper spatial learning and memory formation [38,39,41], LTP responses were analyzed in hippocampuses of control and MMIO rats. Our data showed a significant decrease in LTP magnitudes for rats gestated from hypothyroxinemic mothers, as compared to controls (Fig. 4B). Because input/output curves are consistent with an operative pathway for synaptic excitability of the Schaffer collateral (Fig. 4A), it is seem unlikely that hypothyroxinemia impairs directly the LTP mechanism. Instead, it is possible that hypothyroxinemia could prevent MMIO rats from reaching an LTP level equivalent to that observed for control animals. These results suggest that the diminished LTP could cause low cognitive performance in rats gestated from hypothyroxinemic mothers.

We found significant differences in the content of some proteins that are important for LTP and are located at the PSDs of glutamatergic synapses, such as PSD-95, NR1, and TrkB. In contrast the content of actin, P75, TrkA, CAMKII, NR2A and/or NR2B showed no significant differences between MMIO and control animals (Fig. 5A). A striking increase in the expression and aggregation of the scaffolding protein PSD-95 was observed in the MMIO group. We tested whether abnormal PSD-95 content could alter the NMDA receptor location and the content at the PSD. Although the content of NR1 and NR2A/B subunits at the PSDs were similar between MMIO and control animals, an accumulation of NR1 was observed in the hippocampal (Fig.6). In addition, an excess of PSD-95 could alter the signal transduction pathway triggered by NMDA activation. This alteration in the signal

transduction pathway could impair the increase of phosphorylated c-Fos required for the assembly of a stable AP-1 complex and for the learning process. Finally, it is likely that overexpression of PSD-95 in the MMI group could alter the dendrite stability, as described for immature neurons [42]. Dendrite stability and synapses are modulated both by PSD-95 and TrkB [42-44]. The small but significant increase of TrkB at the PSD and total telencephalon homogenate supports the notion that synapse stability could be impaired in the offspring of hypothyroxinemic mothers.

In conclusion, we found an increase of PSD-95 and TrkB in the PSD of MMIO. Alterations in the protein composition of the PSD in the telencephalon could be responsible for reduced synaptic function. Because the PSD is responsible for neurotransmitters reception and for postsynaptic response, changes in PSD protein composition could affect the synaptic function of these neurons. Consequently, mechanisms like LTP could be deteriorated affecting cognitive processes like spatial memory.

Here we present new and novel evidence supporting the notion that maternal hypothyroxinemia affects the central nervous system of the offspring, which is in conceptual agreement with previous studies [6-10]. We have shown that cognition in rats was affected in the same manner as in humans and that this damage persisted to adulthood. We reported detrimental changes in the LTP performance of this offspring and observed changes of protein composition in the PSD of these animals. These cellular and molecular findings underscore the reduced spatial learning abilities of the MMI offspring. Better knowledge of the molecular process that underlies the cognitive damage caused by maternal hypothyroxinemia can encourage clinicians to search early for this condition in pregnant women.

Understanding the molecular deficiencies underlying learning disabilities could contribute to ultimately design new therapy alternatives for this condition. Considering that commonly maternal hypothyroxinemia is caused by an insufficient iodine intake by pregnant or lactating women, it is feasible that alterations caused by this condition could be prevented by a

daily administration of KI supplement (200 µg of iodine) during pregnancy. This harmless procedure might possibly contribute to the full potential neurodevelopment of the fetus and the newborn [45].

ACKNOWLEDGMENTS

We are grateful to Drs. Robert J. Wenthold for anti-NR1 and NR2 A/B subunits antibodies and Francisca Bronfman for the anti-TrkA antibody. We would like to thank Drs. Nancy Carrasco and Diane O'Dwod, as well as Susannah Volpe

for critically reading the manuscript. This work was supported by FONDECYT grants 1040349; 1070352 and ICM P04/030-F. PAG is a fellow from CONICYT Chile.

REFERENCES

1. **Morreale de Escobar, G, Obregon, MJ Escobar del Rey F** 2000 Is neuropsychological development related to maternal hypothyroidism or to maternal hypothyroxinemia? *J Clin Endocrinol Metab* 85: 3975-87
2. **Glinoeer D, Delange F** 2000 The potential repercussions of maternal, fetal, and neonatal hypothyroxinemia on the progeny. *Thyroid* 10: 871-87
3. **Vermiglio F, Lo Presti VP, Moleti M, Sidoti M, Tortorella G, Scaffidi G, Castagna MG, Mattina F, Violi MA, Crisa A, Artemisia A, Trimarchi F.** 2004 Attention deficit and hyperactivity disorders in the offspring of mothers exposed to mild-moderate iodine deficiency: a possible novel iodine deficiency disorder in developed countries. *J Clin Endocrinol Metab* 89: 6054-60
4. **Kooistra L, Crawford S, van Baar AL, Brouwers EP, Pop VJ** 2006 Neonatal effects of maternal hypothyroxinemia during early pregnancy. *Pediatrics* 117: 161-7
5. **Kasatkina EP, Samsonova LN, Ivakhnenko VN, Ibragimova GV, Ryabykh AV, Naumenko LL, Evdokimova YA** 2006 Gestational hypothyroxinemia and cognitive function in offspring. *Neurosci Behav Physiol* 36: 619-24
6. **Pop VJ, Kuijpers JL, van Baar AL, Verkerk G, van Son MM, de Vijlder JJ, Vulsma T, Wiersinga WM, Drexhage HA, Vader HL** 1999 Low maternal free thyroxine concentrations during early pregnancy are associated with impaired psychomotor development in infancy. *Clin Endocrinol (Oxf)* 50: 149-55
7. **Pop VJ, Brouwers EP, Vader HL, Vulsma T, van Baar AL, de Vijlder JJ** 2003 Maternal hypothyroxinaemia during early pregnancy and subsequent child development: a 3-year follow-up study. *Clin Endocrinol (Oxf)* 59: 282-8
8. **Lavado-Autric R, Auso E, Garcia-Velasco JV, Arufe Mdel C, Escobar del Rey F, Berbel P, Morreale de Escobar G** 2003 Early maternal hypothyroxinemia alters histogenesis and cerebral cortex cytoarchitecture of the progeny. *J Clin Invest* 111: 1073-82
9. **Auso E, Lavado-Autric R, Cuevas E, Del Rey FE, Morreale De Escobar G, Berbel P** 2004 A moderate and transient deficiency of maternal thyroid function at the beginning of fetal neocortico-genesis alters neuronal migration. *Endocrinology* 145: 4037-47
10. **Cuevas E, Auso E, Telefont M, Morreale de Escobar G, Sotelo C, Berbel P** 2005 Transient maternal hypothyroxinemia at onset of corticogenesis alters tangential migration of medial ganglionic eminence-derived neurons. *Eur J Neurosci* 22: 541-51
11. **Guzowski JF** 2002 Insights into immediate-early gene function in hippocampal memory consolidation using antisense oligonucleotide and fluorescent imaging approaches. *Hippocampus* 12: 86-104
12. **Fleischmann A, Hvalby O, Jensen V, Strekalova T, Zacher C, Layer LE, Kvello A, Reschke M, Spanagel R, Sprengel R, Wagner EF, Gass P** 2003 Impaired long-term memory and NR2A-type NMDA receptor-dependent synaptic plasticity in mice lacking c-Fos in the CNS. *J Neurosci* 23: 9116-22
13. **Gass P, Fleischmann A, Hvalby O, Jensen V, Zacher C, Strekalova T, Kvello A, Wagner EF, Sprengel R** 2004 Mice with a fra-1 knock-in into the c-fos locus show impaired spatial but regular contextual learning and normal LTP. *Brain Res Mol Brain Res* 130: 16-22
14. **Teather LA, Packard MG, Smith DE, Ellis-Behnke RG, Bazan NG** 2005 Differential induction of c-Jun and Fos-like proteins in rat hippocampus and dorsal striatum after training in two water maze tasks. *Neurobiol Learn Mem* 84: 75-84

15. **Correa da Costa VM, Rosenthal D** 1996 Effect of aging on thyroidal and pituitary T4-5'-deiodinase activity in female rats. *Life Sci* 59: 1515-20
16. **Biebinger R, Arnold M, Langhans W, Hurrell RF, Zimmermann MB** 2007 Vitamin A repletion in rats with concurrent vitamin A and iodine deficiency affects pituitary TSHbeta gene expression and reduces thyroid hyperstimulation and thyroid size. *J Nutr* 137: 573-7
17. **Gorski JR, Rozman K**, 1987 Dose-response and time course of hypothyroxinemia and hypoinsulinemia and characterization of insulin hypersensitivity in 2,3,7,8-tetrachlorodibenzo-p-dioxin (TCDD)-treated rats. *Toxicology* 44: 297-307
18. **Morris R** 1984 Developments of a water-maze procedure for studying spatial learning in the rat. *J Neurosci Methods* 11: 47-60
19. **Carlin R, Grab D, Cohen R, Siekevitz P** 1980 Isolation and characterization of postsynaptic densities from various brain regions: enrichment of different types of postsynaptic densities. *J Cell Biol* 86: 831-843
20. **Smith PK, Krohn RI, Hermanson GT, Mallia AK, Gartner FH, Provenzano MD, Fujimoto EK, Goeke NM, Olson BJ, Klenk DC** 1985 Measurement of protein using bicinchoninic acid. *Anal Biochem* 150: 76-85
21. **Blahos J, Wenthold RJ** 1996 Relationship between N-methyl-D-aspartate receptor NR1 splice variants and NR2 subunits. *J Biol Chem* 271: 15669-74
22. **Roux PP, Colicos MA, Barker PA, Kennedy TE** 1999 p75 neurotrophin receptor expression is induced in apoptotic neurons after seizure. *J Neurosci* 19: 6887-96
23. **Kornau HC, Schenker LT, Kennedy MB, Seeburg PH** 1995 Domain interaction between NMDA receptor subunits and the postsynaptic density protein PSD-95. *Science* 269: 1737-40
24. **Muller D, Djebbara-Hannas Z, Jourdain P, Vutskits L, Durbec P, Rougon G, Kiss JZ** 2000 Brain-derived neurotrophic factor restores long-term potentiation in polysialic acid-neural cell adhesion molecule-deficient hippocampus. *Proc Natl Acad Sci U S A* 97: 4315-20
25. **Murray SS, Perez P, Lee R, Hempstead BL, Chao MV** 2004 A novel p75 neurotrophin receptor-related protein, NRH2, regulates nerve growth factor binding to the TrkA receptor. *J Neurosci* 24: 2742-9
26. **Patton BL, Molloy SS, Kennedy MB** 1993 Autophosphorylation of type II CaM kinase in hippocampal neurons: localization of phospho- and dephosphokinase with complementary phosphorylation site-specific antibodies. *Mol Biol Cell* 4: 159-72
27. **Pezet S, Marchand F, D'Mello R, Grist J, Clark AK, Malcangio M, Dickenson AH, Williams RJ, McMahon SB** 2008 Phosphatidylinositol 3-kinase is a key mediator of central sensitization in painful inflammatory conditions. *J Neurosci* 28: 4261-70
28. **Greenberg ME, Ziff EB** 1984 Stimulation of 3T3 cells induces transcription of the c-fos proto-oncogene. *Nature* 311: 433-8
29. **Szapacs ME, Mathews TA, Tessarollo L, Ernest Lyons W, Mamounas LA, Andrews AM** 2004 Exploring the relationship between serotonin and brain-derived neurotrophic factor: analysis of BDNF protein and extraneuronal 5-HT in mice with reduced serotonin transporter or BDNF expression. *J Neurosci Methods* 140: 81-92
30. **Eugenin EA, Berman JW** 2003 Chemokine-dependent mechanisms of leukocyte trafficking across a model of the blood-brain barrier. *Methods* 29: 351-61
31. **Deng T, Karin M** 1994 c-Fos transcriptional activity stimulated by H-Ras-activated protein kinase distinct from JNK and ERK. *Nature* 371: 171-5
32. **Bannister AJ, Brown HJ, Sutherland JA, Kouzarides T** 1994 Phosphorylation of the c-Fos and c-Jun HOB1 motif stimulates its activation capacity. *Nucleic Acids Res* 22: 5173-6

33. **Treisman R** 1996 Regulation of transcription by MAP kinase cascades. *Curr Opin Cell Biol* 8: 205-15
34. **Morris RG, Anderson E, Lynch GS, Baudry M** 1986 Selective impairment of learning and blockade of long-term potentiation by an N-methyl-D-aspartate receptor antagonist, AP5. *Nature* 319:774-6
35. **Lynch MA** 2004 Long-term potentiation and memory. *Physiol Rev* 84: 87-136
36. **Collingridge GL, Kehl SJ, McLennan H** 1983 Excitatory amino acids in synaptic transmission in the Schaffer collateral-commissural pathway of the rat hippocampus. *J Physiol* 334: 33-46
37. **Li XL, Aou S, Oomura Y, Hori N, Fukunaga K, Hori T** 2002 Impairment of long-term potentiation and spatial memory in leptin receptor-deficient rodents. *Neuroscience* 113: 607-15
38. **Yaka R, Salomon S, Matzner H, Weinstock M** 2007 Effect of varied gestational stress on acquisition of spatial memory, hippocampal LTP and synaptic proteins in juvenile male rats. *Behav Brain Res* 179: 126-32
39. **Wozniak DF, Xiao M, Xu L, Yamada KA, Ornitz DM** 2007 Impaired spatial learning and defective theta burst induced LTP in mice lacking fibroblast growth factor 14. *Neurobiol Dis* 26: 14-26
40. **Morris RG, Garrud P, Rawlins JN, O'Keefe J** 1982 Place navigation impaired in rats with hippocampal lesions. *Nature* 297: 681-3
41. **Barco A, Bailey CH, Kandel ER** 2006 Common molecular mechanisms in explicit and implicit memory. *J Neurochem* 97: 1520-33
42. **Charych EI, Akum BF, Goldberg JS, Jornsten RJ, Rongo C, Zheng JQ, Firestein BL** 2006 Activity-independent regulation of dendrite patterning by postsynaptic density protein PSD-95. *J Neurosci* 26: 10164-76
43. **Ehrlich I, Klein M, Rumpel S, Malinow R** 2007 PSD-95 is required for activity-driven synapse stabilization. *Proc Natl Acad Sci U S A* 104: 4176-81
44. **Ji Y, Pang PT, Feng L, Lu B** 2005 Cyclic AMP controls BDNF-induced TrkB phosphorylation and dendritic spine formation in mature hippocampal neurons. *Nat Neurosci* 8: 164-72
45. **Berbel P, Obregon MJ, Bernal J, Escobar del Rey F, Morreale de Escobar G** 2007 Iodine supplementation during pregnancy: a public health challenge. *Trends Endocrinol Metab* 18: 338-43

Figure 1: Methimazole treatment induced hypothyroxinemia in pregnant rats.

Plasmatic levels of fT_4 , tT_3 , and TSH in pregnant rats treated with MMI or not (control). Rats at E12 were treated with MMI for 4 d and on the last day of treatment (E15) a blood sample was taken from these animals and the control group to measure the TSH and thyroid hormone levels (see Materials and Methods). (A) Mean values for fT_4 levels (ng/dl) \pm SEM of MMI and control rats (n=6) were plotted. (B) Mean values for tT_3 levels (ng/dl) \pm SEM of MMI and control rats (n=6) were plotted. (C) Mean values for TSH levels \pm SEM of MMI (n=3) and control rats (n=4) were plotted. Significant differences were observed only at the levels of fT_4 among control and MMI rats ($P < 0.05$).

Figure 2: Mean escape latency in the water maze test.

(A) Rats gestated in hypothyroxinemic mothers (MMIo) and control rats (Co) were subjected for 5 d to a water maze test. Each of the rats performed five trials. Each trial consisted of positioning the rat in the pool and recording the time that the rat required to reach the hidden platform (see Materials and Methods). The day of each trial is indicated on the x-axis and the mean \pm SE escape latency for every group is indicated on the y-axis. The mean escape latency is the average of 5 trials performed in that day for all rats of the same experimental group. Empty circles (\circ) show the mean \pm SE escape latency for the Co (n=17); black circles (\bullet) show the mean \pm SE latencies for MMIo (n=16). Statistical analysis (Mann-Whitney) shows significant differences on days 2, 3, and 4 with a $P < 0.05$. (B) Control (Co) (n=3) and MMI offspring (MMIo) (n=3) were subjected for 3 d consecutive to water maze test with a visible platform. The day of each trial is indicated on the x-axis and the mean \pm SE escape latency for every group is indicated on the y-axis. The mean escape latency is the average of 5 trials performed in 1 d for all rats of the same experimental group. Statistical analysis (unpaired t -test) shows no significant differences between control and MMIo group.

Figure 3: Content of c-Fos and phosphorylated c-Fos in the telencephalon of rats gestated in hypothyroxinemic mothers.

(A) Representative pictures of western blots for c-Fos and phosphorylated c-Fos (phospho c-Fos) from total telencephalon homogenates. These samples corresponded to total telencephalon homogenate of MMIo or control group (Co) subjected (+) or not (-) to a water maze test on the second day. To analyze that the same amount of protein was loaded in each well, a western blot analysis of actin was performed with the same nitrocellulose used for c-Fos and phospho c-Fos antibodies. (B) Ratio of c-Fos or phosphorylated c-Fos (phospho c-Fos) of rats subjected to water maze test over those that were not subjected to water maze test. The intensities of c-Fos or phospho c-Fos bands from the western blots were measured by densitometry. The ratios between the intensity of c-Fos or phospho c-Fos bands of rats subjected to water maze test over those that were not were plotted. The statistics analysis indicated that the Co increased the content of phospho c-Fos after the second day of water maze test $N=3$, $P < 0.05$.

Figure 4: Effect of maternal hypothyroxinemia over Schaffer collateral – CA1 synaptic function of their progeny.

(A) Input-output (I/O) curves display the mean fEPSP amplitude + SEM for control (\bullet) and MMIo (\circ) rat hippocampal slices. At least three different animals were used for each experimental condition. (B) Effect of maternal hypothyroxinemia over LTP induction of their progeny. Mean fEPSP amplitude + SEM obtained from slices of control rats (\bullet) and MMIo rats (\circ). At least three different animals were used for each experimental condition. (C) The traces correspond to fEPSP measured in the *stratum radiatum* of representative experiments for each condition (control (Co) and MMIo) before TBS (gray line) and 30 min after TBS (black line).

Figure 5: Expression of postsynaptic density proteins in the total telencephalon homogenate and PSD fractions of rats gestated in hypothyroxinemic mothers.

Total telencephalon homogenate and PSD were prepared from MMIo group or Co group. About 20 μ g of PSD and 40 μ g of homogenate were loaded in a SDS-PAGE gel, separated by electrophoresis, were electrotransferred to nitrocellulose, and were analyzed by western blots. The figure shows representative westerns blots performed for six

different proteins of the PSD. Each western blot was repeated three times, each time with three independent samples. Every sample used each time corresponding to a pool of 10 animals. A western blot of actin was used as loaded control. **(B)** BDNF content in the telencephalon of rats gestated in hypothyroxinemic mothers. The telencephalon was isolated, homogenized, and subjected to BDNF determination (see Materials and Methods). BDNF was quantified and its concentration was normalized against the total amount of protein in the sample. BDNF from rats gestated in hypothyroxinemic mothers was termed (MMIo) and BDNF from control rats was termed (Co). The values represent the means \pm SE of six independent experiments. Student's *t*-test (unpaired) yielded $P>0.05$.

Figure 6: NR1 and PSD-95 localization in the hippocampus of rats gestated in hypothyroxinemic mothers.

The NR1 and PSD-95 colocalization were analyzed in CA1 area of the hippocampus of MMIo or control groups by confocal microscopy. **A** and **E** show DAPI staining (blue), for nucleus identification at CA1 area. **B** and **F** show NR1 staining (FITC, green). **C** and **G** show PSD-95 staining (Cy3, red). **D** and **H** show the merger of the three fluorochromes DAPI, FITC, and Cy3, to analyze the colocalization of NR1 and PSD-95. Bar: $5\mu\text{m}$. **A**, **B**, **C**, and **D** correspond to confocal microscopy pictures of the control group. **E**, **F**, **G**, and **H** correspond to confocal microscopy pictures of the MMIo group.

Figure 1

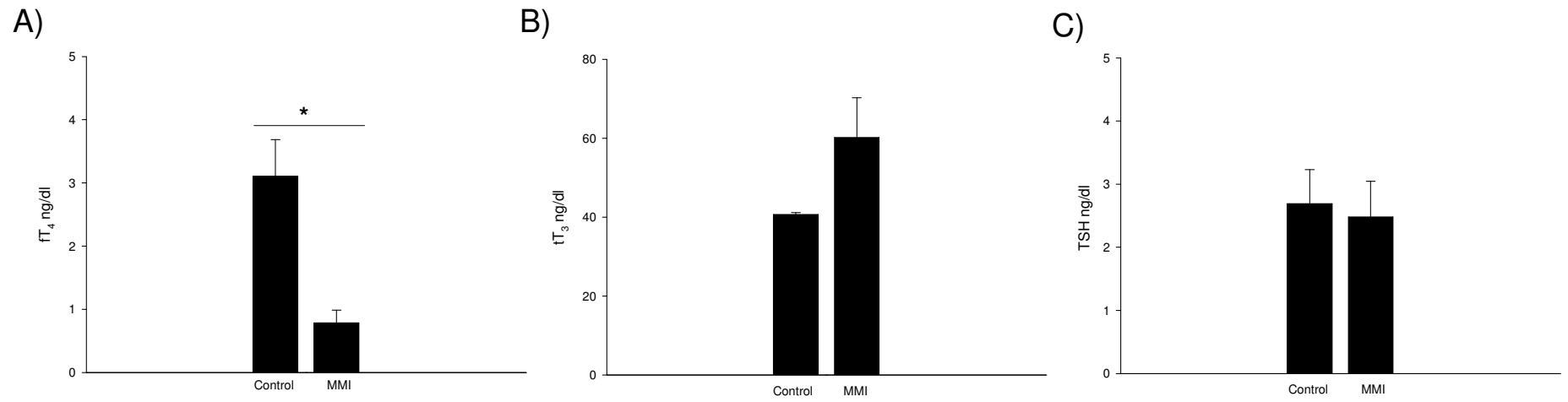


Figure 2A

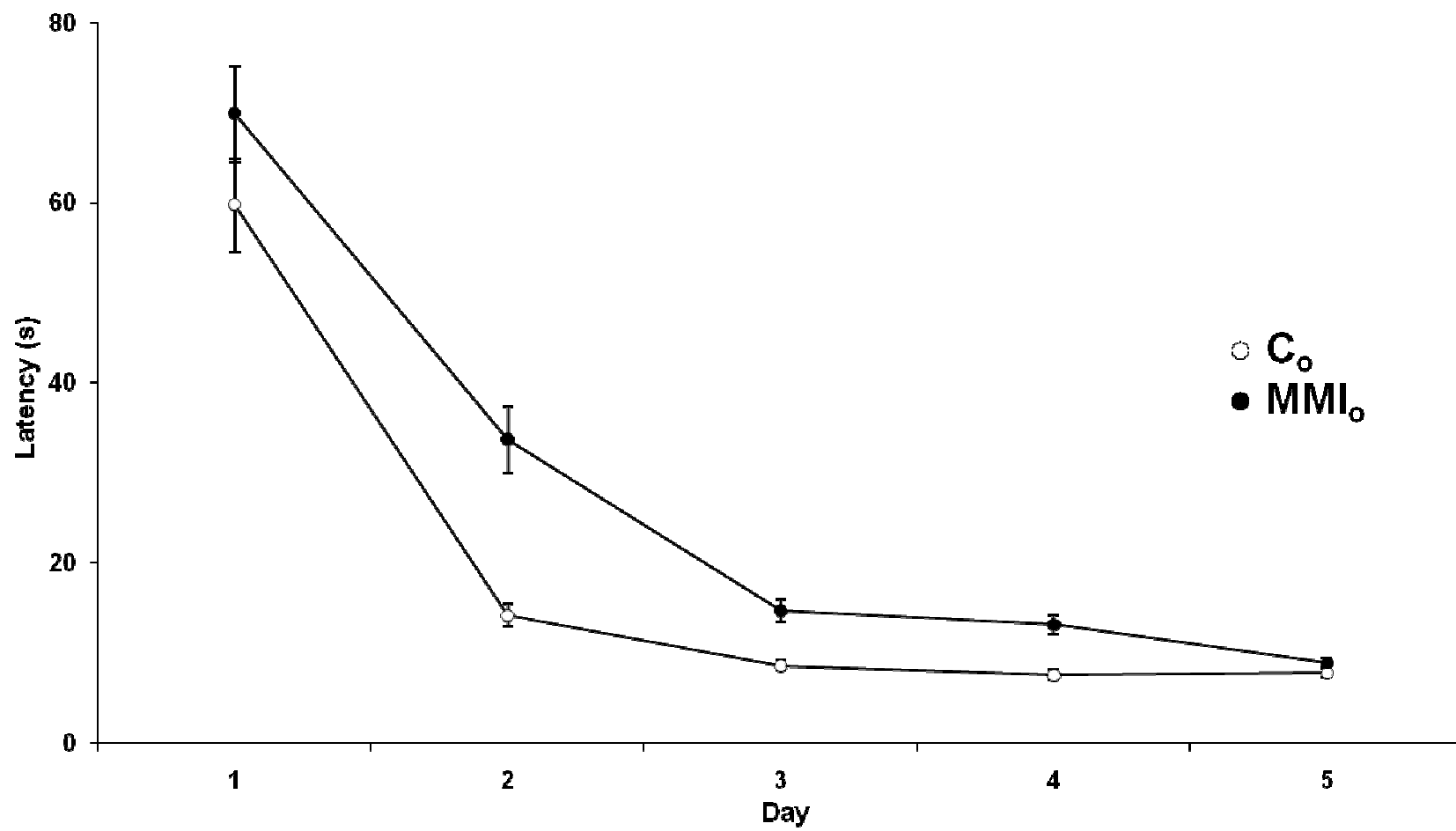


Figure 2B

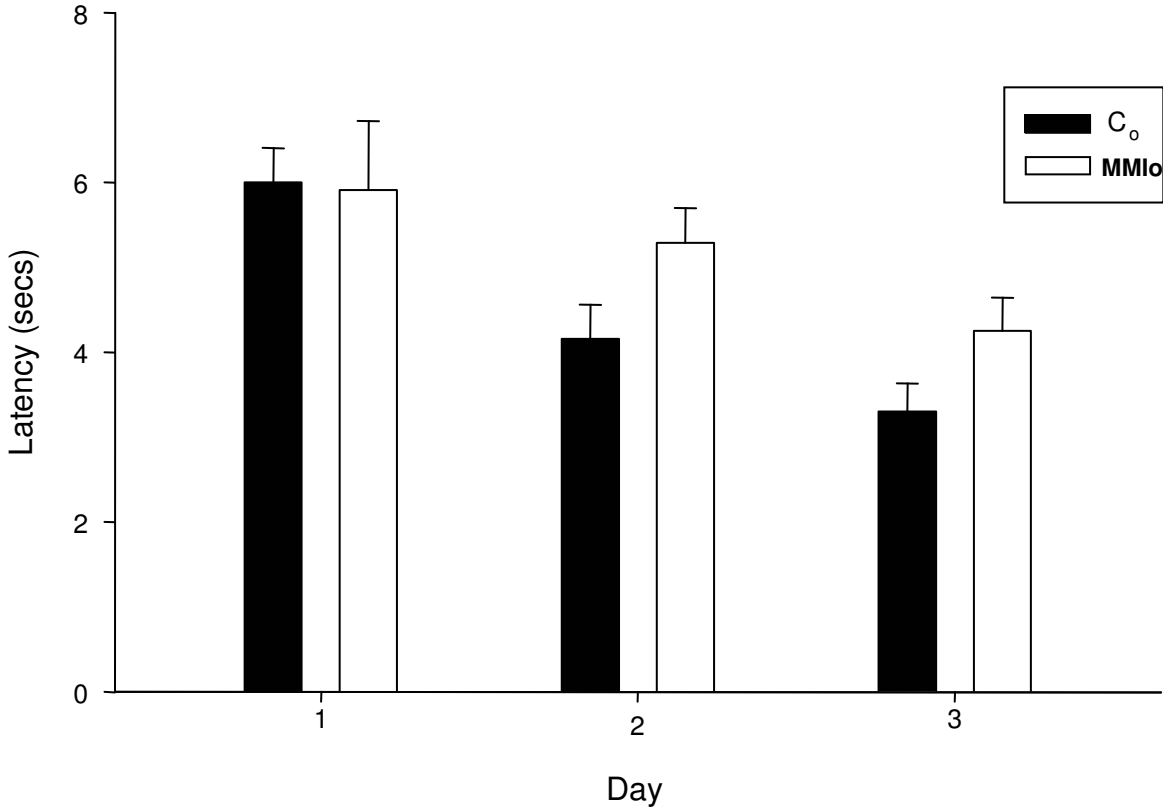


Figure 3A

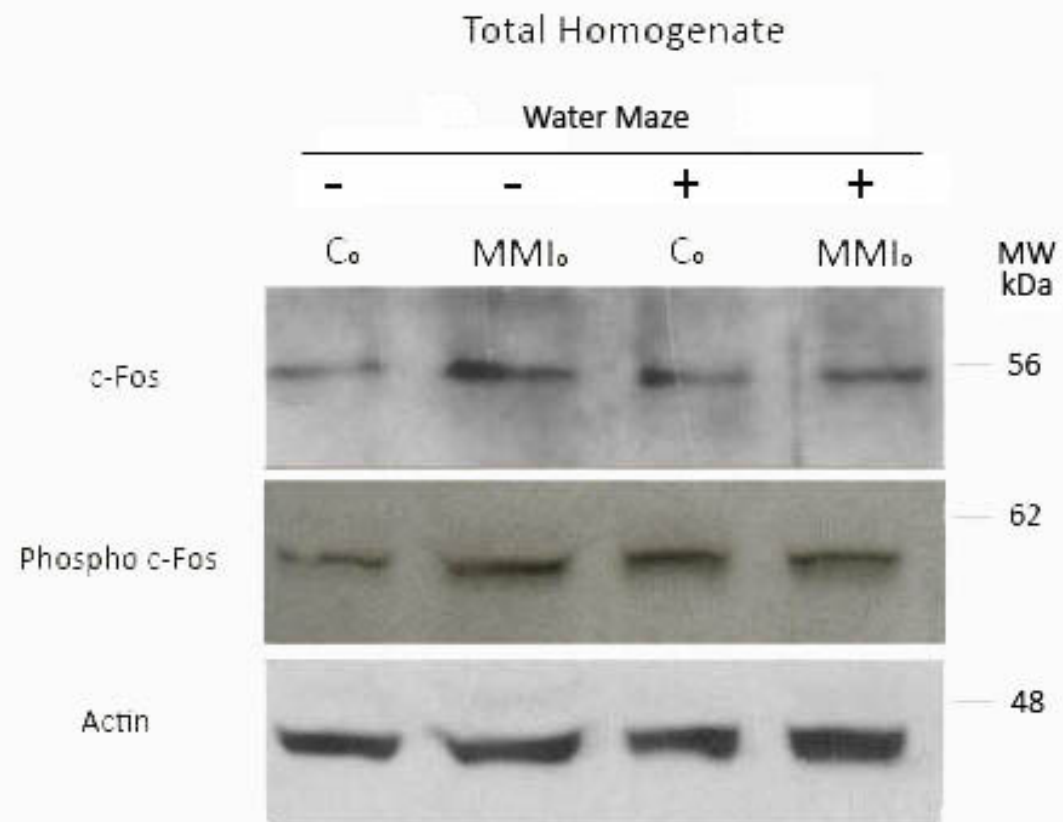


Figure 3B

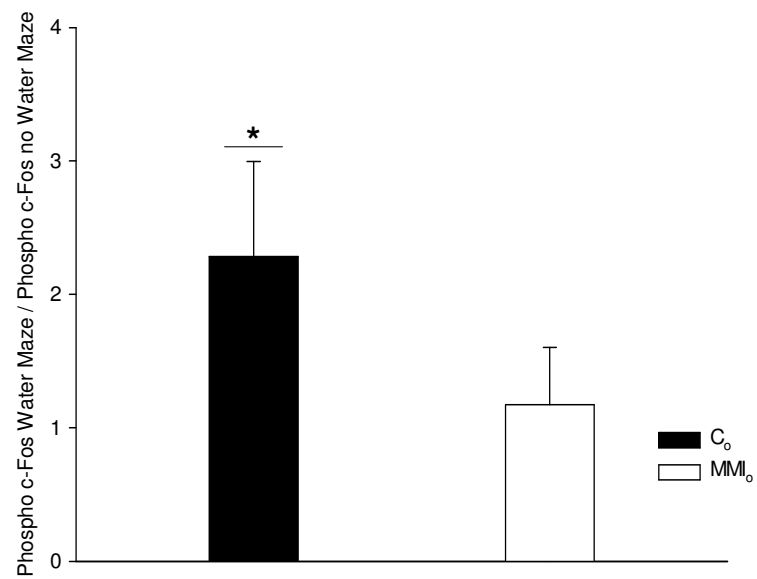
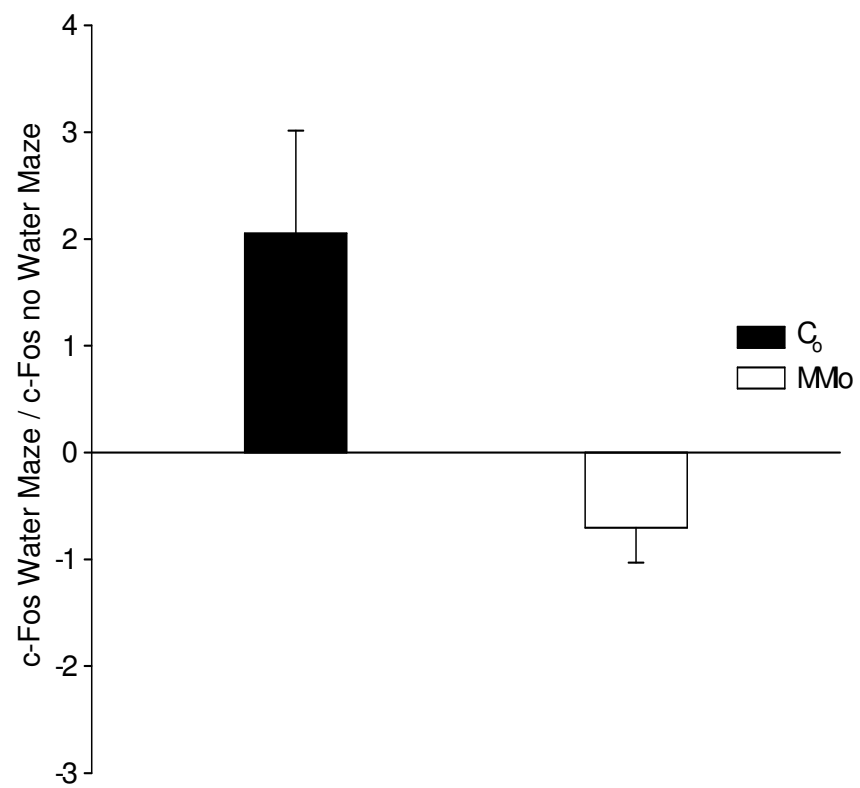


Figure 4A

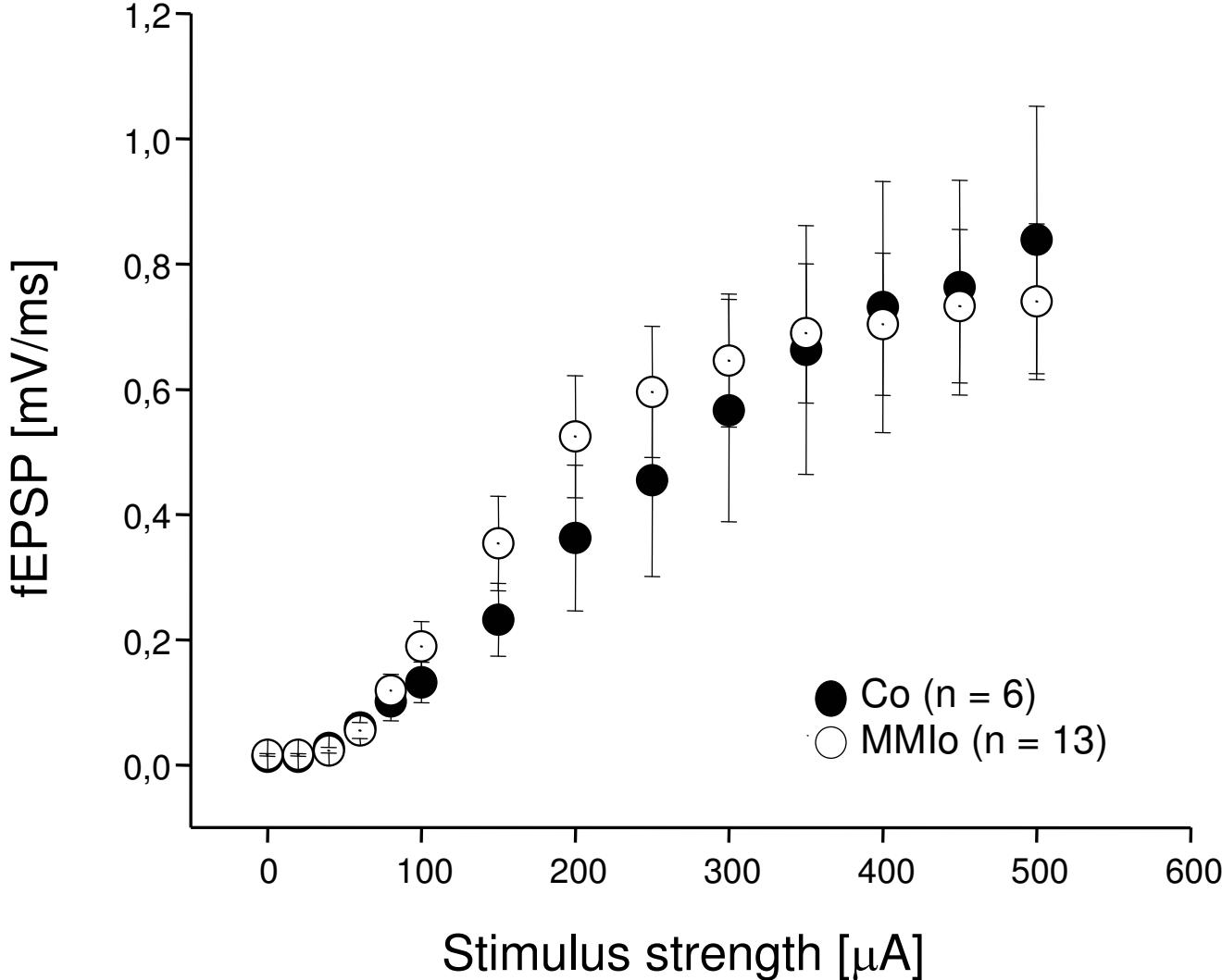


Figure 4B

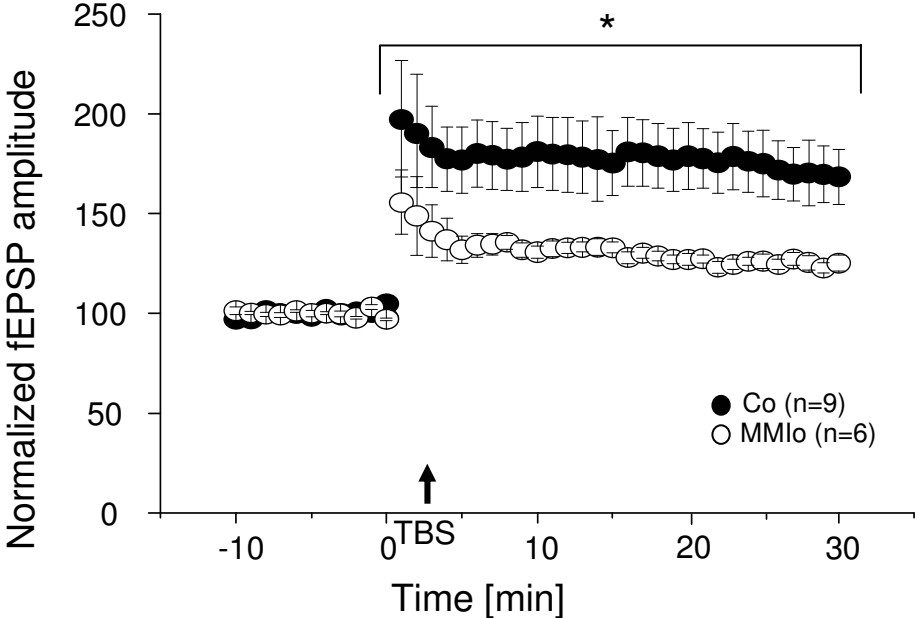


Figure 4C

C

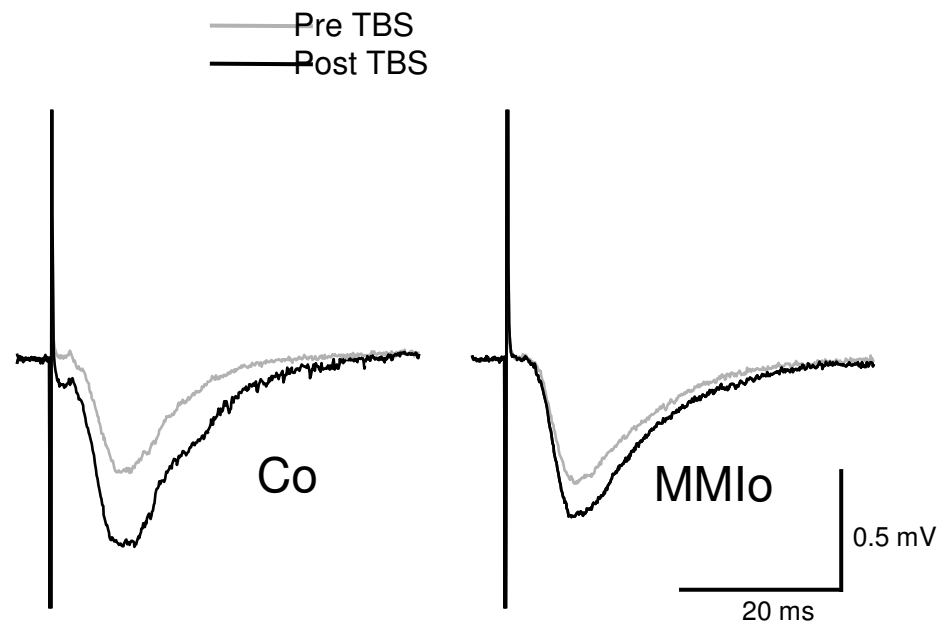


Figure 5A

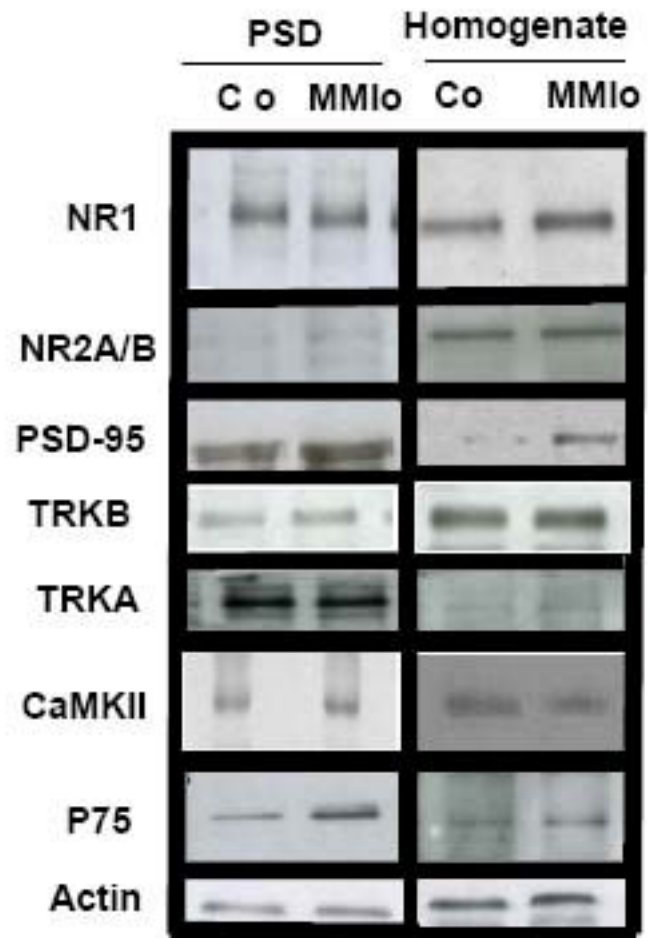


Figure 5B

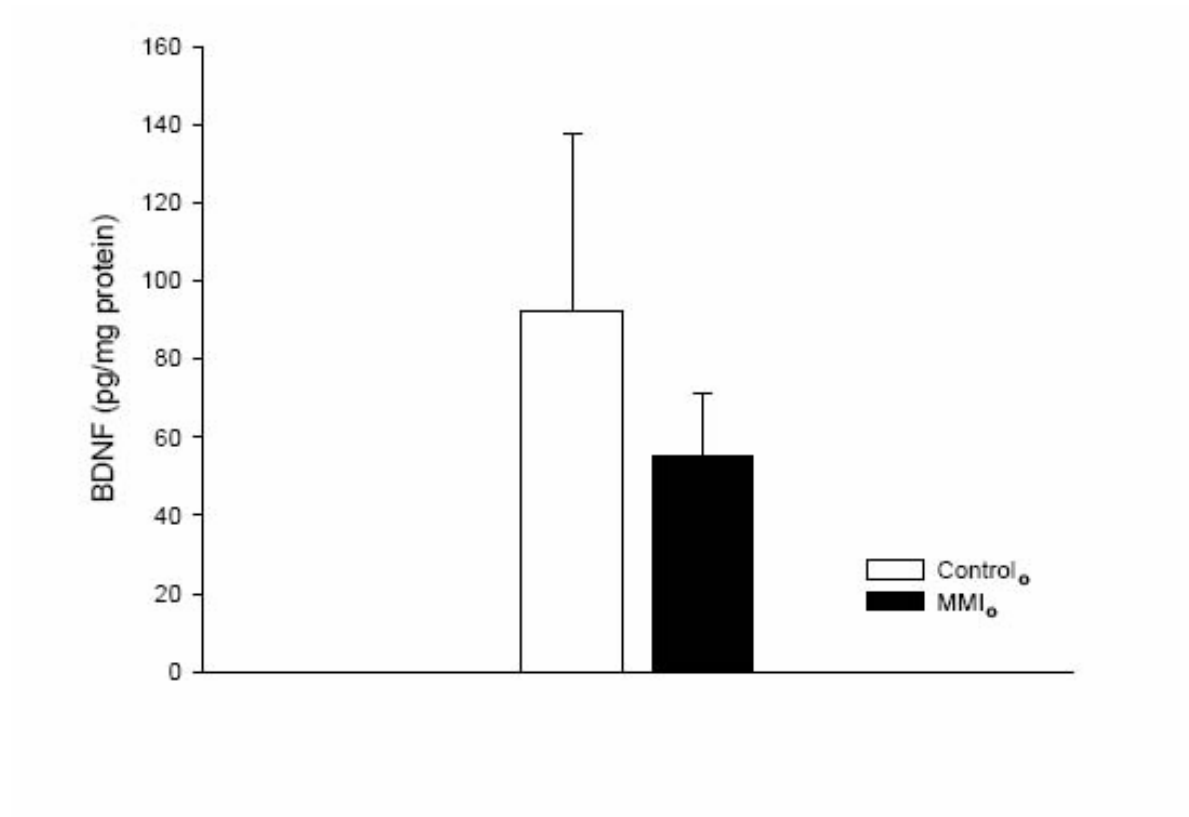


Figure 6

